# Indoor 3D Localization with Low-Cost LiFi Components

E.W. Lam and T.D.C. Little

Department of Electrical and Computer Engineering

Boston University, 8 Saint Mary's St., Boston, MA 02215 USA

(617) 353-9877

*tdcl@bu.edu*

**Abstract:** Indoor positioning or localization is an enabling technology expected to have a profound impact on mobile applications. Various modalities of radio frequency, acoustic, and light can be used for localization; in this paper we consider how visible light positioning can be realized for 3D positioning as a service comprised of optical sources part of an overarching lighting infrastructure. Our approach, called Ray-Surface Positioning, uses one or more overhead luminaires, modulated as LiFi, in conjunction with a steerable laser to realize position estimates in three dimensions.

In this paper, we build and demonstrate Ray-Surface Positioning using low-cost commodity components in a test apparatus representing one quadrant of a 4 m x 4 m x 1 m volume. Data are collected at regular intervals in the test volume representing 3D position estimates and is validated using a motion capture system. For the low-cost components used, results show position estimate errors of less than 30 cm for 95% of the test volume. These results, generated with commodity components, show the potential for 3D positioning in the general case. When the plane of the receiver is known a priori, the position estimate error diminishes to the resolution of the steering mechanism.

**Keywords:** LiFi, Visible Light Communications (VLC) and Positioning (VLP), 2D and 3D Positioning, Location Based Services (LBS).

# 1   Introduction

Optical wireless communications has taken a turn in recent years toward visible light and diffuse sources in what is called Visible Light Communications (VLC). VLC was initially introduced to address and and alleviate the increasing bandwidth crunch in the data downlink in RF networks [1]. With this new focus on VLC, other use cases for VLC besides network communications have also emerged. One such use case is for indoor positioning, which when realized with light becomes Visible Light Positioning (VLP) [2]. Indoor positioning or indoor localization is an emerging field with numerous competing technologies beyond visible light, including RF, acoustic, and imaging [3]. The excitement about indoor positioning is due to the likelihood that the winning technology will drastically alter and influence the localization landscape the same way the Global Navigation Satellite System (GNSS) has done with outdoor applications.

VLP fares favorably amongst its competitors in that it leverages preexisting infrastructure (lighting) to provide positioning services. This is a common characteristic with LiFi, which can also exploit lighting. Thus both technologies are sensible from cost and deployment perspectives.

VLP solutions typically require an active photodiode on the target (mobile) device to achieve positioning. This is in contrast to systems that detect passive objects or gestures. An advantage of this approach is the ability for the target to decide to participate or opt out of positioning which can be attractive from a privacy standpoint. Fig. 1 shows a broad schema in which VLP is used to position in 3D robots, personal devices, smart devices, and emerging technologies such as augmented and virtual realty headsets.
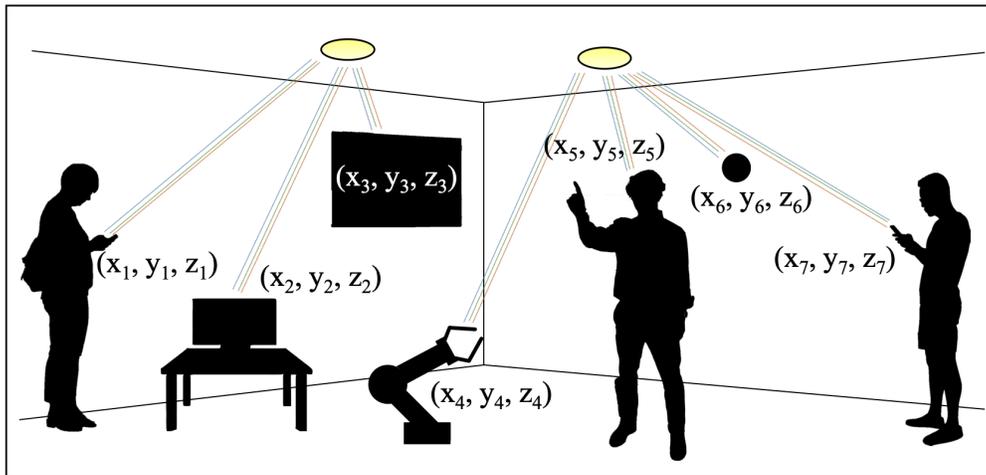


Figure 1: 3D indoor localization of various types of devices using a light-based infrastructure

Most VLP solutions use trilateration (multilateration) or triangulation as a core method to establish position estimates. However, the performance qualifications of these techniques in 3D positioning are sparse and sometimes impossible due to the physical field-of-view limitations of both the luminaire (transmitter) and photodiode (receiver) in 3D [4]. The

limits on FOV impact the line-of-sight (LOS) access to luminaires, which is troublesome when multiple luminaires are required for positioning. In the most recent literature, researchers augment lighting with added peripherals, such as additional PDs [5,6], steerable lasers [7], and even rotating receivers [8] to eliminate the need to position with more than one luminaire while still providing 3D positioning. These added peripherals also increase positioning accuracies particularly if they add angular diversity [4].

Our contribution to VLP is in the concept of Ray-Surface Positioning (RSP). This technique combines angular information from a steerable beam with ranging information derived from the isointense envelope from one or more luminaires as detected at a receiver [7]. In this paper, we describe a first implementation of RSP to validate theoretical and simulated predictions on 3D positioning accuracy.

We build out an end-to-end experimental apparatus consisting of two sources: a narrow beam (laser) and a Lambertian (luminaire); and a receiver with a single photodiode. We collect data from our build and show promising results for RSP. This experimental build not only validates the capability of RSP but also gives us good working knowledge on how to better improve the next iteration.

The remainder of the paper is organized as follows: Section 2 briefly describes Ray-Surface Positioning; Section 3 details the experimental apparatus; and Section 4 discusses the results of experiments and future prospects. Finally, Section 5 concludes the paper.

## 2    Ray-Surface Positioning

RSP combines a narrow optical emission and a wide diffuse emission to position an active receiver, such as a photodiode, in a 3D space relative to the sources. In this section, we briefly describe the RSP method, a concept introduced with analytical and simulation results in our previous paper [7], and how to solve for position using said methodology. RSP is characterized by the two components in its name: a ray and a surface. In light-based positioning, the "ray" is a narrow steerable laser beam continuously-encoded (modulated) with its pointing angle. When a receiving photodiode detects the laser signal, it decodes the modulated signal to glean angle with respect to the receiver position. The geometry of these angles, $\theta_{laser}$ and $\phi_{laser}$, are shown in Fig. 2. The location of the sources are known a priori or, alternatively, can be communicated along with the laser angles.

The other component in RSP is the "surface." A Lambertian source with a wide FOV works well in providing an isointense surface that is a function of the distance the photodiode is from the Lambertian and also the normal angles of the photodiode and luminaire, Fig. 2. This Lambertian surface is defined with the following line-of-sight (LOS) channel [9,10]:

$$H_{LOS}^{DC} = \begin{cases} \frac{A}{d^2} R_{eff}(\psi) \frac{m+1}{2\pi} cos^m(\phi) cos(\psi), & 0 \leq \psi \leq \Psi \\ 0, & \psi > \Psi \end{cases}, \tag{1}$$

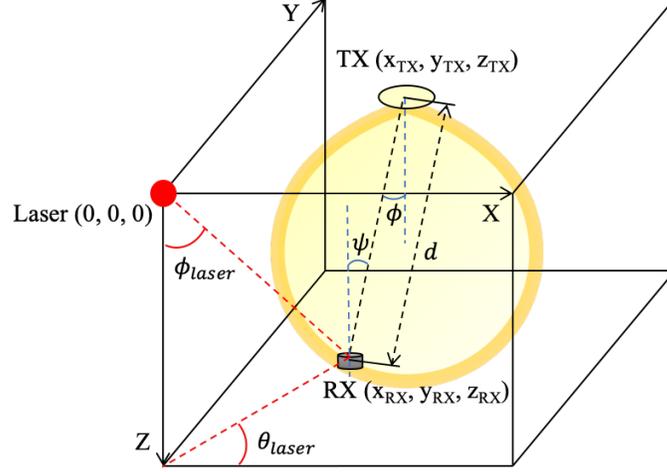where $\Psi$ is the receiver FOV, $A$ is the detector area, $\psi$ is the angle of incidence with respect to

3

Figure 2: Ray-Surface Positioning geometry showing the laser at origin, the Lambertian source and its isointense curve, and a receiver

the receiver axis, $\phi$ is angle of radiance, $d$ is distance between the photodiode and luminaire, $R_{eff}(\psi)$ is the effective responsivity of the photodiode, and $m$ is the Lambertian order of the luminaire based on the semiangle of the luminaire, $\Phi_{1/2}$:

$$m = -\left[\frac{ln(2)}{ln(cos(\Phi_{1/2}))}\right]. \tag{2}$$

At the receiver, the photodiode measures the received-signal-strength (RSS), which is transmitted power attenuated by the channel model, $H_{LOS}^{DC}$, plus noise:

$$P_r = P_t H_{LOS}^{DC} + w, \tag{3}$$

To solve for position, we calculate a ray or line of potential RSS values using Eq. 3 with no added noise based on the received angles at the receiver from the laser, $\theta_{laser}$ and $\phi_{laser}$. Since each point on the line can be described by a unique height and set of angles, we simplify the representation to relying only on height:

$$RSS_{x,y,z} = \begin{bmatrix} RSS(z_1) & RSS(z_2) & ... & Rss(z_K) \end{bmatrix}. \tag{4}$$

The noisy received signal, $P_r$, is then compared to every point on this ideal line, where the index of the smallest deviation corresponds to the position of the photodiode. It is possible that the ray intersects with the surface in two places, resulting in two indices to choose from. In a noiseless situation, it is impossible to distinguish the double intersection points from each other without an additional luminaire to assist. However, in a noisy scenario, there is enough variation in the signal that by taking the $N$ smallest error deviations, a clustering algorithm can be applied to determine two unique clusters so that the cluster with the most points of the $N$ deviations can be taken as the intersection point of interest. Finally, the

mean positions of the cluster are taken as the predicted index value for Z, $z_{pred}$. X and Y are predicted based on $z_{pred}$, $\theta_{laser}$, and $\phi_{laser}$:

$$x_{pred} = z_{pred} \tan \phi_{laser} \sin \theta_{laser}, \tag{5}$$

$$y_{pred} = z_{pred} \tan \phi_{laser} \cos \theta_{laser}. \tag{6}$$

Because RSP only needs one luminaire to position, in a room with multiple luminaires, RSP benefits from always using the luminaire with the strongest signal. This is in contrast to multilateration, which requires more than one luminaire to position regardless of the signal fidelity. For RSP, laser and luminaire redundancy will instead improve signal reliability during occlusions and positioning speed instead of base functionality, e.g., in a space of three luminaires, RSP can still position if LOS to a luminaire is lost. For multilateration, a loss of one luminaire is detrimental. As mentioned above, additional luminaires are also highly beneficial in resolving the ambiguity created when there is a double intersection of the surface. RSP effectively 3D positions with as few as one luminaire and one laser, relying on angle diversity from the laser and RSS diversity from the Lambertian. This combined sources setup augments the pros and compensates the cons of each respective source type.

# 3    Experimental Apparatus

In order to demonstrate our RSP scheme and illustrate its potential as an easy and cost-effective solution to indoor positioning, we build an end-to-end experimental setup. There are three key modules to the RSP apparatus decomposed as follows: the steerable laser (ray), the Lambertian source (surface), and the mobile receiver (target). Fig. 3 shows a block diagram for these three modules and Table 1 shows the exact components chosen for the setup and their respective specifications and cost.

## 3.1    Steerable Laser

At this stage of our RSP development we are most interested in position estimate error and use low-cost servomechanisms for pointing. Later we will optimize for micro-electro-mechanical systems (MEMS)-based steering (e.g., [11]). The implication of this decision is a reduction in the target acquisition time for the current prototype, i.e., positioning is limited to slower-moving targets. We use an ESP32 microcontroller to provide actuation of the two servos, for pan and tilt, and modulation of a transistor-transistor-logic (TTL) laser.

Because the ESP32 is a two core microcontroller, it allows for real-time concurrent tasks: modulating the laser and actuating the servos. In this macro-setup, the pulse-width-modulated (PWM) servos provide the main steering functionality of the laser. As mentioned above, in future builds, we will switch to MEMS, which are capable of fast (kHz) and precise steering of laser sources [11]. In RSP, the modulated laser is used to send the
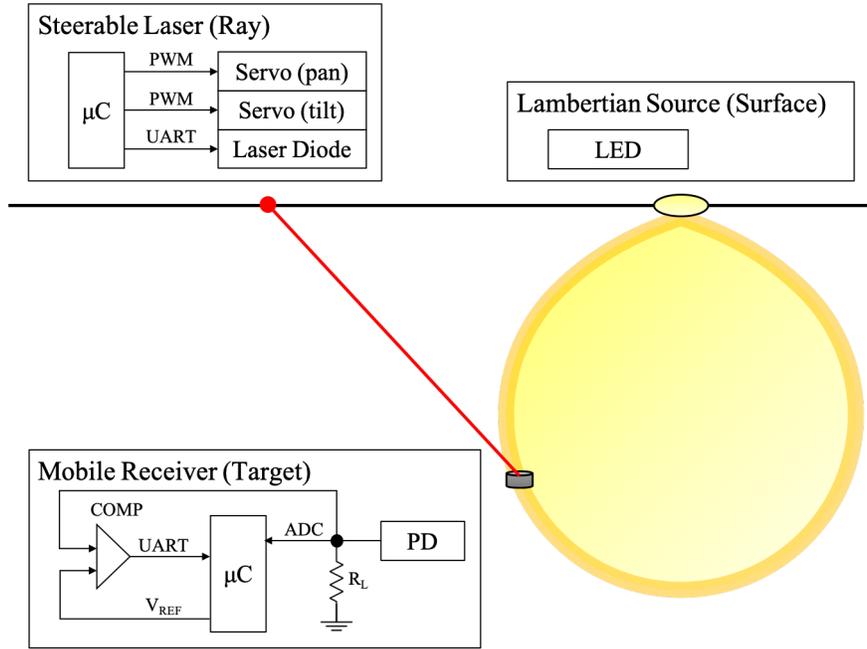
Figure 3: Block diagram showing the three main modules of Ray-Surface Positioning: steerable laser, Lambertian source, and the mobile receiver

angles of the laser. We choose an on-off-keying (OOK)-based modulation protocol adapted to work with the ESP32 universal asynchronous receiver-transmitter (UART) to encode the pointing angles. OOK facilitates simple modulation and demodulation. We also choose a modest baud rate of 115200 to accommodate low-cost receiver circuity. Future builds will incorporate faster modulation; and of course, prior VLC work has shown data rates of Gbps are feasible [12].

## 3.2  Lambertian Source

For the Lambertian source, we use a CREE XLamp MC-E Color LED, which is comprised of four individual LED chips: red, green, blue, and white. The MC-E is a standard component LED available from many vendors. The MC-E has a FOV of 115°, which corresponds to $m = 1.12$ per Eq. 2. With 350 mA provided to each LED, the MC-E can provide a total of 206 lumens, which is about 400 mW after converting from photometric units to radiometric units. However, we do not rely on this specification and instead measure and calibrate the system to obtain actual transmitter power when computing the Lambertian model. The MC-E is also not sufficiently powerful to illuminate a space by itself and has additional faults that we will discuss in the following sections, but it is a good initial single-package LED for us to demonstrate the potential of RSP. In future work we will consider lighting fixtures with multiple LEDs for stronger signal strength and better illumination coverage.

Table 1: Experimental Configurations

| *Module* Parameter | Value |
| --- | --- |
| *Steerable Laser (Ray)* | |
| Laser | Generic TTL, 5 mW, 650 nm |
| Laser Position (x,y,z) | (0 m, 0 m, 0 m) |
| Microcontroller | ESP32 |
| Pan Servo | Savox SV1257MG |
| Tilt Servo | Savox SH0264MG |
| Total Cost | $121 |
| *Lambertian Source (Surface)* | |
| LED | CREE XLamp MC-E Color |
| TX Position (x.y,z) | (1 m, 1 m, 1 m) |
| Lamertian order, $m$ | 1.12 |
| Total Cost | $10 |
| *Receiver (Target)* | |
| Photodiode | Osram KOM 2125 |
| Active Area | 4 mm$^2$ |
| Sensitivity | 0.62 A/W |
| Semiangle, $\Psi$ | 60° |
| Resistive Load, $R_L$ | 510 $k\Omega$ |
| Microcontroller | ESP32 |
| Total Cost | $24 |

## 3.3   Mobile Receiver

The receiver is designed to receive both the modulated laser signal as well as the signal intensity from the luminaire. As such, we split the signal into two inputs: feeding one to a comparator to ensure an on/off digital signal within the voltage range of the ESP32 and feeding the other into the 12-bit resolution analog-to-digital converter (ADC) on the ESP32. We use a reference voltage of 1.1 V, which corresponds to a 0.3 mV resolution. We use a simple voltage divider circuit in series with a photodiode, the Osram KOM 2125, to convert received optical power to electrical current and then to electrical voltage within the range of the ADC. Since this is a simple voltage divider, the speed of the photodiode is limited to the internal capacitance of the photodiode and the resistive load of the voltage divider. Alternatively, a transimpedance amplifier can be used for improved performance at higher complexity.
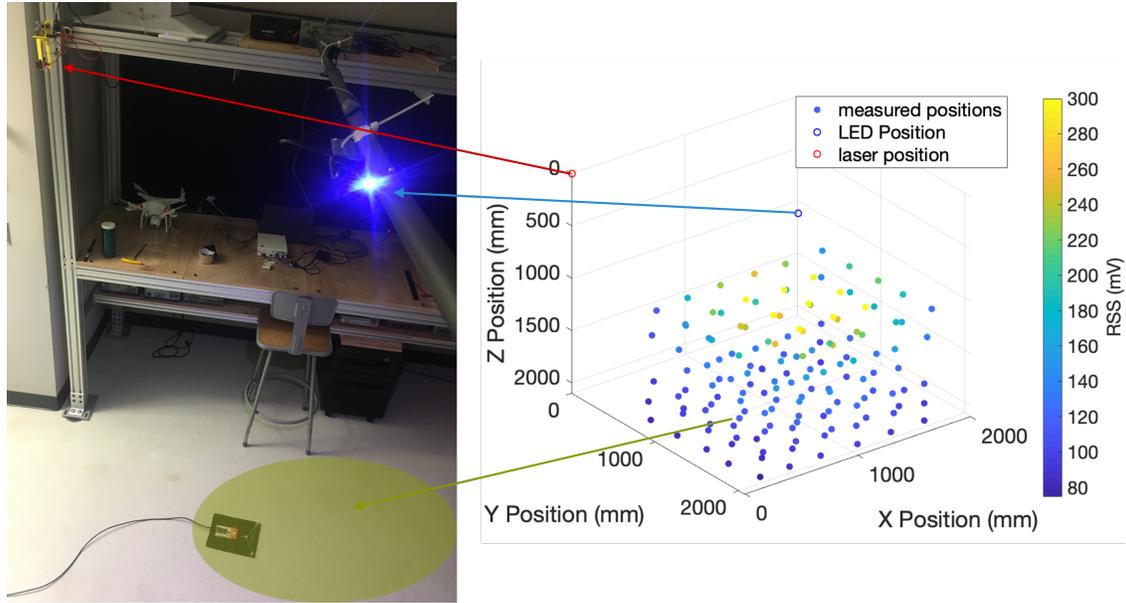
Figure 4: Experimental setup on left with mean RSS data collected at 150 points on right. Reference X and Y-coordinates are obtained from Optitrack.
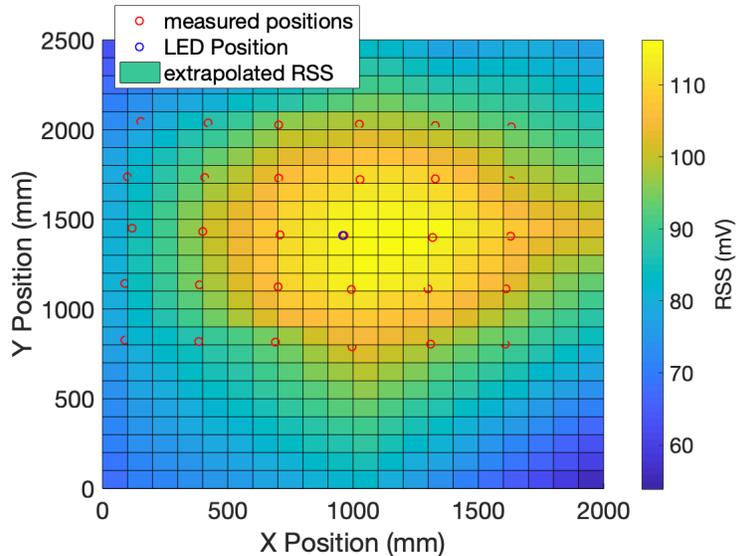


Figure 5: RSS for a horizontal cross-section 2m away from LED (floor)

## 3.4  Data Collection

For data collection, we use a Motion Capture (MoCap) camera system, Optitrack, to obtain our reference position coordinates. The Optitrack system is a high-quality IR camera system that requires prior calibration. We use 8 IR 120 fps cameras (Prime 13) and retroreflective markers to tag our photodiode. The Optitrack systems tracks in 3D a rigidbody associated with the markers to sub-millimeter accuracy. By tagging our receiver with the retroreflective markers, we bypass the need to precisely place the receiver at predetermined locations; we can
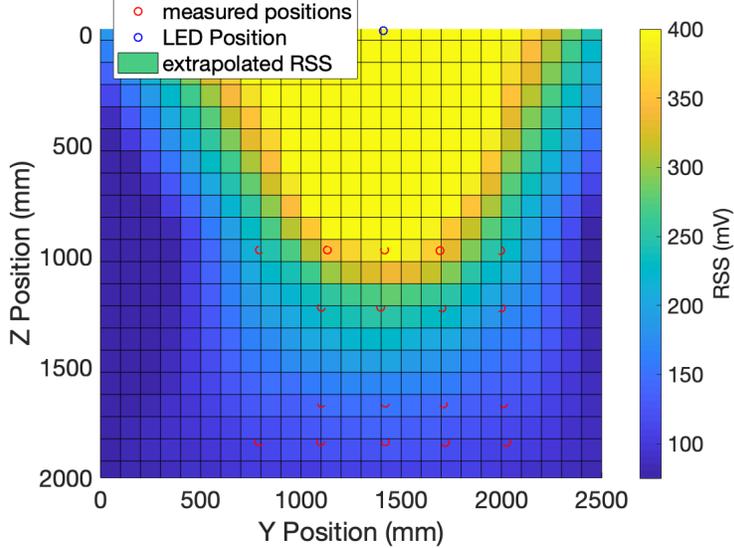
Figure 6: RSS for a vertical cross-section at the LED location

arbitrarily place the receiver and refer to Optitrack measurements for its actual coordinate. The Optitrack resolution is much greater than the RSP resolution and removes human errors in measuring the reference positions.

We collect data at 30 locations on 5 different planes representing a 3D volume, which is a more comprehensive dataset than a plane. At each location, we collect 5 samples of RSS values, a 12-bit resolution received signal voltage, the received angle from the modulated laser signal, and the position from Optitrack. This is a total of 750 points. The mean of the samples at each position is taken as the RSS of that position. Fig. 4 shows the three modules and also the collected RSS values (according to the colorbar) as well as the locations of the receiver, luminaire, and laser.

Fig. 5 and Fig. 6 show cross-sections, xy-plane at the floor and yz-plane down the center of the luminaire respectively, of the collected data linearly interpolated between measured points and extrapolated beyond measured points. As expected, the areas of low signal strength are the locations far from the receiver or are at larger angles from the receiver or both. Fig. 6 shows clearly that angle between the Lambertian and receiver contributes significantly to signal attenuation, because even though distance away from the receiver is small, RSS near the transmitter at larger angles is diminished due to the nature of the Lambertian cosine function. In addition, Fig. 5 also shows that the MC-E exhibits a shifted (to larger x-coordinates) Lambertian coverage; this is due to the nature of the MC-E being constructed using four discrete LEDs. This also means that the sensitivity at the photodiode is different for different wavelengths originating from the individual LEDs.

9

# 4    Results and Discussion

In the following we discuss the experimental results of our prototype system and observations as we consider the next iteration of the concept implementation. Our main concern is the expected position estimate error bound. In prior work, we predicted a bound of less than 10cm within 95% of the measured volume. However, for the prototype we experienced error of within 10cm at 70% of the bound (or less than 30 cm within 95% of the volume). We address ways to address this discrepancy below and as considerations for future experiments.

## 4.1    2D Positioning Errors

2D positioning error is related to the steering resolution, which is unfortunately lacking for the inexpensive servos used in the experiments. This is an area for improvement. In an ideal scenario with perfect steering, there would be no errors in 2D [7]. However, we found the servos highly unreliable in steering and the beam-width of the laser too narrow to reliably land on the target photodiode. When the beam lands, transmission of the angle is seamless. From a small experimental dataset, on average, there is an error of 2.6° for $\theta_{laser}$ and 1.3° for $\phi_{laser}$. We found measuring angles cumbersome and use these errors to simulate the angles with measured RSS values for the 3D position estimates (below). We found that whether the angles were perfect or noisy made little difference on position estimates as RSS is still the noise-dominant signal. This indifference in angle precision motivates us to pursue larger beam widths in our next iteration so that targeting is easier without loss of accuracy. MEMs-based steering will also combat the unreliability of macro servos and 3D printed mounts.

## 4.2    3D Positioning Errors

Using the error angles mentioned in the previous section and measured RSS values, we calculate position estimates in 3D using RSP, as described in Section 2. Fig. 7 shows the actual positions in comparison to the position estimates. The errors are larger for smaller x-positions, which is due to the MC-E having a shifted coverage, which is seen in Fig. 5. Errors are also greater in those sections because the RSS from the transmitter is weaker the further the photodiode is away from the transmitter. Fig. 8 gives the cumulative distribution function (CDF) of the errors. The 95% coverage error is about 30cm for each of the three dimensions. These positioning accuracies are lower but comparable to the reported positioning accuracy of simulated RSP [7].
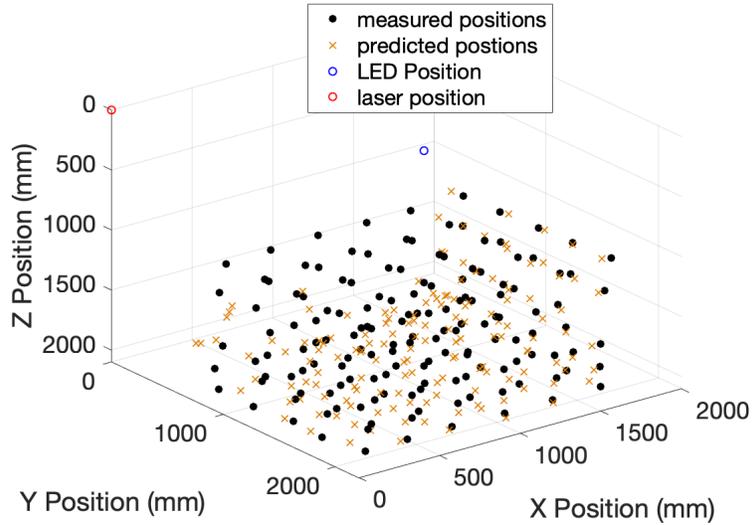
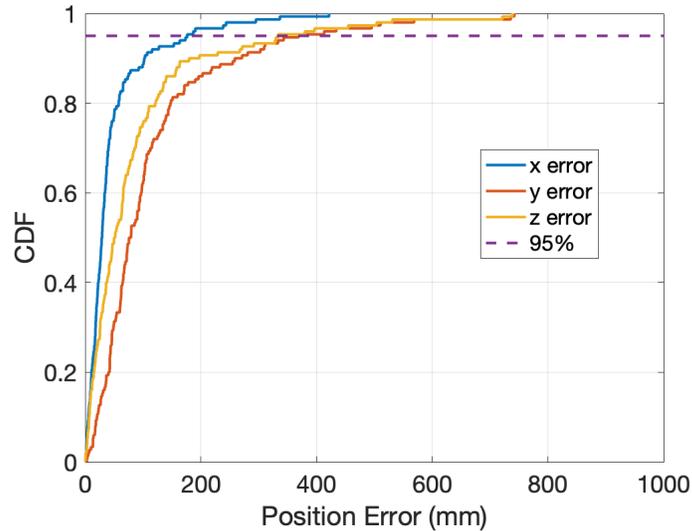Figure 7: 3D positioning: actual positions versus position estimates



Figure 8: CDF of positioning errors

## 4.3  Discussion and Future Considerations

There are a variety of future directions that we are exploring for RSP. These are described below.

### 4.3.1  One Light Source

RSP only requires one luminaire to position. This is an important distinction because for 3D positioning, LOS to the photodiode is not always available due to blockage by various

objects including a user's head. The angle diversity is provided by the laser and can be augmented to the system without affecting lighting conditions. If luminaires are placed to optimize VLP, the overall lighting would be unconventional. It is also easier to steer lasers than depend on other noisy farther-distanced Lambertians or steer other clunky Lambertian sources to obtain the same angle diversity introduced by a steerable laser.

### 4.3.2   Redundant Sources

Since only one light source is used for RSP, the additional luminaires in a space can be used for redundancy. The added redundancy will aid in occlusions, an important shortcoming of LOS systems. Lasers can also be placed redundantly through a space.

### 4.3.3   Real-Time Optical Communications

RSP actively uses real-time VLC to aid in positioning. This strategy is different than traditional VLC which is used for transmitting data as a network link. VLC enables real-time angle synchronization and association between the laser and photodiode. This is a unique methodology to provide angular diversity and system configurations via communication without an RF backhaul.

### 4.3.4   Eye Safety

For low speed communications, which are sufficiently fast but not at the bandwidth for streaming rich media content, low-power and eye-safe lasers can easily provide enough power for modulation through a typical office space (e.g., a simple laser pointer device) as demonstrated by our prototype. In addition, since the laser is not used for lighting, it can also use invisible light, i.e., IR. The steerable laser is an inexpensive means to provide angle diversity in an indoor positioning system.

### 4.3.5   Future Builds

The described low cost experimental system demonstrates an error bound within 10cm at 70% of the measured volume (or less than 30 cm within 95% of the volume). We anticipate improved error performance in subsequent builds with more robust components. Future implementations will be realized using MEMS beam steering for more accuracy, speed, and a smaller footprint. In addition, we expect to evaluate RSP using our VLC testbed comprised of an array of commercial-off-the-shelf lighting fixtures (troffers) to establish performance from non-point-source lighting. The shifted coverage of the MC-E is also problematic in this build deviating from a standard Lambertian. Our next build will use a more conventional Lambertian and also brighter source to give better signal strength and coverage in a large

space. We would also work at reducing as much noise as possible, e.g., calibrating for temperature variances. Finally, we would like to prototype using multiple luminaires to showcase the advantages of Ray-Surface Positioning in multi-luminaire spaces.

# 5    Concluding Remarks

We demonstrate an end-to-end solution implementing Ray-Surface Positioning (RSP) using low-cost commodity components. In our experimental build, we show positioning accuracy for each of the three dimensions of around 30 cm. Although the errors are larger than the predicted (simulated) errors, the position spread of the errors follow the same pattern as expected (i.e., large errors in regions of weak signal). This suggests that with higher quality components we can more precisely position devices with the proposed method.

RSP incorporates a steerable laser that is capable of communicating through VLC its own angles. This steerable laser provides a distinguished way to obtain angle diversity without compromising luminaire layouts or lighting quality; and without needing complex receivers capable of measuring angle.

Finally, RSP positions in 3D without requiring LOS access to more than one luminaire, which combats FOV limitations due to the physical geometries of the space. This is hardly the case for many VLP schemes. With more than one luminaire, we anticipate RSP to better handle occlusions and poor signal coverage.

# References

[1] H. Elgala, R. Mesleh, and H. Haas, "Indoor optical wireless communication: potential and state-of-the-art," *Communications Magazine, IEEE*, vol. 49, no. 9, pp. 56–62, September 2011.

[2] J. Armstrong, Y. A. Sekercioglu, and A. Neild, "Visible light positioning: a roadmap for international standardization," *IEEE Communications Magazine*, vol. 51, no. 12, pp. 68–73, December 2013.

[3] D. Lymberopoulos and J. Liu, "The microsoft indoor localization competition: Experiences and lessons learned," *IEEE Signal Processing Magazine*, vol. 34, no. 5, pp. 125–140, Sept 2017.

[4] E. W. Lam and T. D. C. Little, "Visible light positioning: Moving from 2D planes to 3D spaces (invited)," *Chinese Optics Letters*, vol. 17, no. 3, p. 030604, Mar 2019. [Online]. Available: http://col.osa.org/abstract.cfm?URI=col-17-3-030604

[5] S. H. Yang, H. S. Kim, Y. H. Son, and S. K. Han, "Three-dimensional visible light indoor localization using aoa and rss with multiple optical receivers," *Journal of Lightwave Technology*, vol. 32, no. 14, pp. 2480–2485, July 2014.

[6] A. Naz, N. U. Hassan, M. A. Pasha, H. Asif, T. M. Jadoon, and C. Yuen, "Single led ceiling lamp based indoor positioning system," in *2018 IEEE 4th World Forum on Internet of Things (WF-IoT)*, Feb 2018, pp. 682–687.

[7] E. W. Lam and T. D. C. Little, "Resolving height uncertainty in indoor visible light positioning using a steerable laser," in *2018 IEEE International Conference on Communications Workshops (ICC Workshops)*, May 2018, pp. 1–6.

[8] Q.-L. Li, J.-Y. Wang, T. Huang, and Y. Wang, "Three-dimensional indoor visible light positioning system with a single transmitter and a single tilted receiver," *Optical Engineering*, vol. 55, pp. 55 – 55 – 7, 2016.

[9] J. Kahn and J. Barry, "Wireless infrared communications," *Proceedings of the IEEE*, vol. 85, no. 2, pp. 265–298, Feb 1997.

[10] T. Komine and M. Nakagawa, "Fundamental analysis for visible-light communication system using led lights," *IEEE Transactions on Consumer Electronics*, vol. 50, no. 1, pp. 100–107, Feb 2004.

[11] J. Morrison, M. Imboden, T. D. C. Little, and D. J. Bishop, "Electrothermally actuated tip-tilt-piston micromirror with integrated varifocal capability," *Optics Express*, vol. 23, no. 7, pp. 9555–9566, Apr 2015. [Online]. Available: https://doi.org/10.1364/OE.23.009555

[12] Y.-C. Chi, D.-H. Hsieh, C.-T. Tsai, H.-Y. Chen, H.-C. Kuo, and G.-R. Lin, "450-nm gan laser diode enables high-speed visible light communication with 9-gbps qam-ofdm," *Opt. Express*, vol. 23, no. 10, pp. 13 051–13 059, May 2015.